



Cite this: *RSC Adv.*, 2024, **14**, 23495

# Synthesis, characterization and biological research of novel 2-(quinoline-4-carbonyl)hydrazide-acrylamide hybrids as potential anticancer agents on MCF-7 breast carcinoma cells by targeting EGFR-TK†

Hany M. Abd El-Lateef,<sup>\*ab</sup> Duaa Bafail,<sup>c</sup> Noura Hamdi Yousef Alhalees,<sup>d</sup> Eslam E. M. Toson,<sup>e</sup> Ali H. Abu Almaaty,<sup>f</sup> Elsherbiny H. Elsayed,<sup>e</sup> Islam Zaki<sup>g</sup> and Magdy M. Youssef<sup>h</sup>

Novel derivatives of the 2-(quinoline-4-carbonyl)hydrazide scaffold carrying the acrylamide moiety were synthesized and tested for their cytotoxic efficacy against the breast carcinoma MCF-7 cell line. The most active members **6a**, **6b** and **6h** revealed significant antiproliferative action with an  $IC_{50}$  value of 3.39, 5.94 and 2.71  $\mu$ M, respectively, which were more potent than the reference drug Dox ( $IC_{50}$  = 6.18  $\mu$ M). Aiming to enlighten the antiproliferative activity, compounds **6a** and **6h** were examined for their inhibitory potential against EGFR kinase. The results demonstrated that compound **6h** displayed potent inhibitory activity, as concluded from the  $IC_{50}$  value ( $IC_{50}$  = 0.22  $\mu$ M) compared to the standard drug Lapatinib ( $IC_{50}$  value of 0.18  $\mu$ M). Compound **6h** was found to induce significant cellular cycle arrest at the G1 phase and provoke apoptosis. Besides, compound **6h** triggered apoptosis via upregulating p53 and initiator caspase 9 by 7.4- and 8.7-fold, respectively, compared to DMSO controls.

Received 29th May 2024  
Accepted 19th July 2024

DOI: 10.1039/d4ra03963g  
[rsc.li/rsc-advances](http://rsc.li/rsc-advances)

## 1. Introduction

Cancer continues to be the most difficult illness to cure and the second-largest cause of death in the world.<sup>1</sup> Despite current therapeutic protocols, the majority of patients acquire drug resistance, develop tumor recurrence metastasis and have low survival rates.<sup>2,3</sup> Therefore, the establishment of novel therapies that are both less harmful and more effective is one of the most intensely pursued goals of contemporary medicinal chemistry.<sup>4,5</sup> Understanding the molecular mechanisms that regulate growth and survival of tumor cells would provide insights into

potential targets for drug design and synthesis.<sup>6,7</sup> Epidermal growth factor receptor (EGFR) is known to be the key regulator of many complex biological processes, including cell motility, cell cycle regulation as well as apoptosis activation and metastasis.<sup>8,9</sup> The aberrant expression of EGFR has been correlated with cancer progression.<sup>10</sup> Recently, reports have shown evidence supporting the overexpression of EGFR in many cancer patients, which indicates that inhibition of EGFR could be beneficial in cancer treatment.<sup>11,12</sup> In addition, many tumors exhibited increased expression of anti-apoptotic factors and decreased expression of apoptotic mediators.<sup>13</sup> For example, caspase 9; an initiator of tumor-mediated apoptosis is expressed at low levels in many tumor cell lines.<sup>14</sup> The modulation of anti-apoptotic and pro-apoptotic gene expression contributes to increased proliferation and survival resulting in tumor growth, suggesting potential as druggable treatment targets.<sup>15</sup>

The biological importance of quinoline derivatives has drawn a lot of attention to their chemistry.<sup>16-18</sup> Quinoline based derivatives displayed cancer fighting properties in many tumor types through EGFR signalling inhibition.<sup>19</sup> In addition, it is well documented that quinoline compounds shown to deplete the proliferation and prompted caspase-dependent death of MCF-7 cell *in vitro*.<sup>20</sup> It also enhances the expression of p53 before apoptosis.<sup>21</sup> These findings point to the quinoline moiety as promising agent for the establishment for the creation of cancer therapy.

<sup>a</sup>Department of Chemistry, College of Science, King Faisal University, Al-Ahsa 31982, Saudi Arabia. E-mail: hmahmed@kfu.edu.sa

<sup>b</sup>Department of Chemistry, Faculty of Science, Sohag University, Sohag 82524, Egypt

<sup>c</sup>Department of Clinical Pharmacology, Faculty of Medicine, King Abdulaziz University, Jeddah, Saudi Arabia

<sup>d</sup>Ministry of Health, King Abdullah Medical Complex, Jeddah, Saudi Arabia

<sup>e</sup>Chemistry Department, Faculty of Science, Port Said University, Port Said 42526, Egypt

<sup>f</sup>Zoology Department, Faculty of Science, Port Said University, Port Said 42526, Egypt

<sup>g</sup>Pharmaceutical Organic Chemistry Department, Faculty of Pharmacy, Port Said University, Port Said, Egypt. E-mail: Eslam.Zaki@pharm.psu.edu.eg

<sup>h</sup>Biochemistry Division, Chemistry Department, Faculty of Science, Mansoura University, Mansoura, Egypt

† Electronic supplementary information (ESI) available. See DOI: <https://doi.org/10.1039/d4ra03963g>



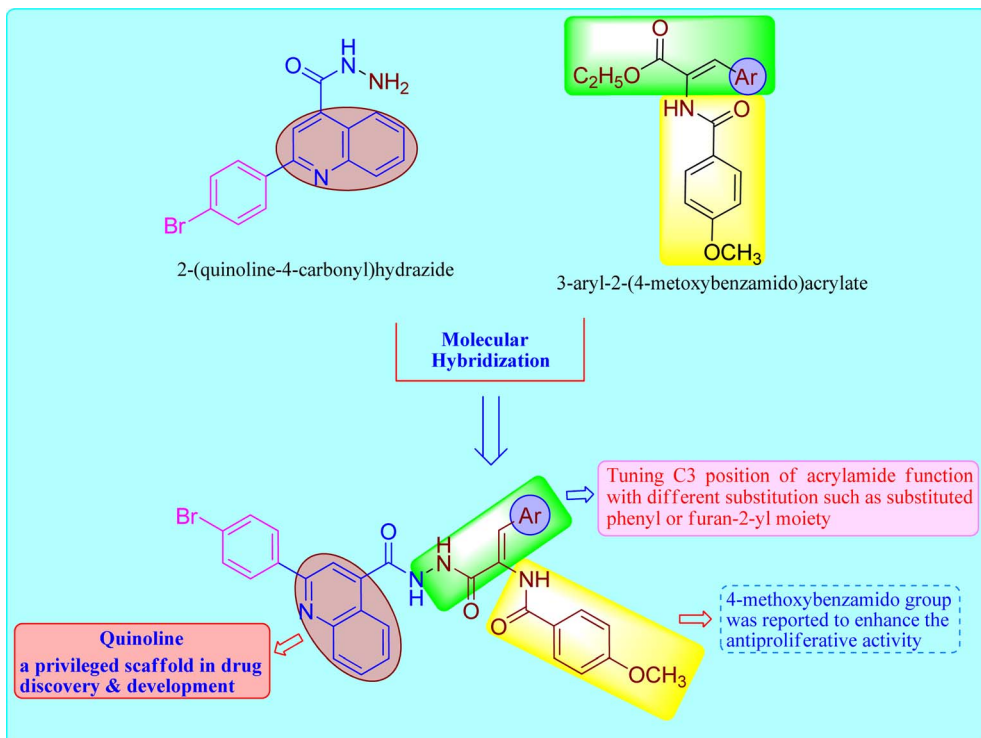


Fig. 1 The design concept used for the synthesis of the title compounds 5 and 6a–i.

In recent years, synthesis of acrylamide derivatives has been regarded of great interest to organic chemistry owing to their therapeutic properties.<sup>22</sup> Acrylamide scaffold exhibited various biological properties including antitumor *via* EGFR tyrosine kinase inhibition.<sup>23</sup> Furthermore, it is also evidenced from literature that quinoline moiety linked to acrylamide function with different substitution pattern possess a wide range of anticancer properties.<sup>24</sup> Many acrylamide containing derivatives were evaluated for their cytotoxic capacity *via* inhibition of EGFR-TK signalling. In addition, acrylamide-based anticancer agents showed great potential for the treatment of cancer by induction of cell cycle arrest, differentiation, and cellular apoptosis.<sup>25,26</sup> Afatinib, an acrylamide-containing drug, is an EGFR kinase inhibitor indicated for the treatment of adult patients with metastatic, non-small lung cancer.<sup>27</sup> It covalently binds to the kinase domain of EGFR and irreversibly inhibits tyrosine kinase autophosphorylation, resulting in down-regulation of EGFR downstream signaling.<sup>28</sup>

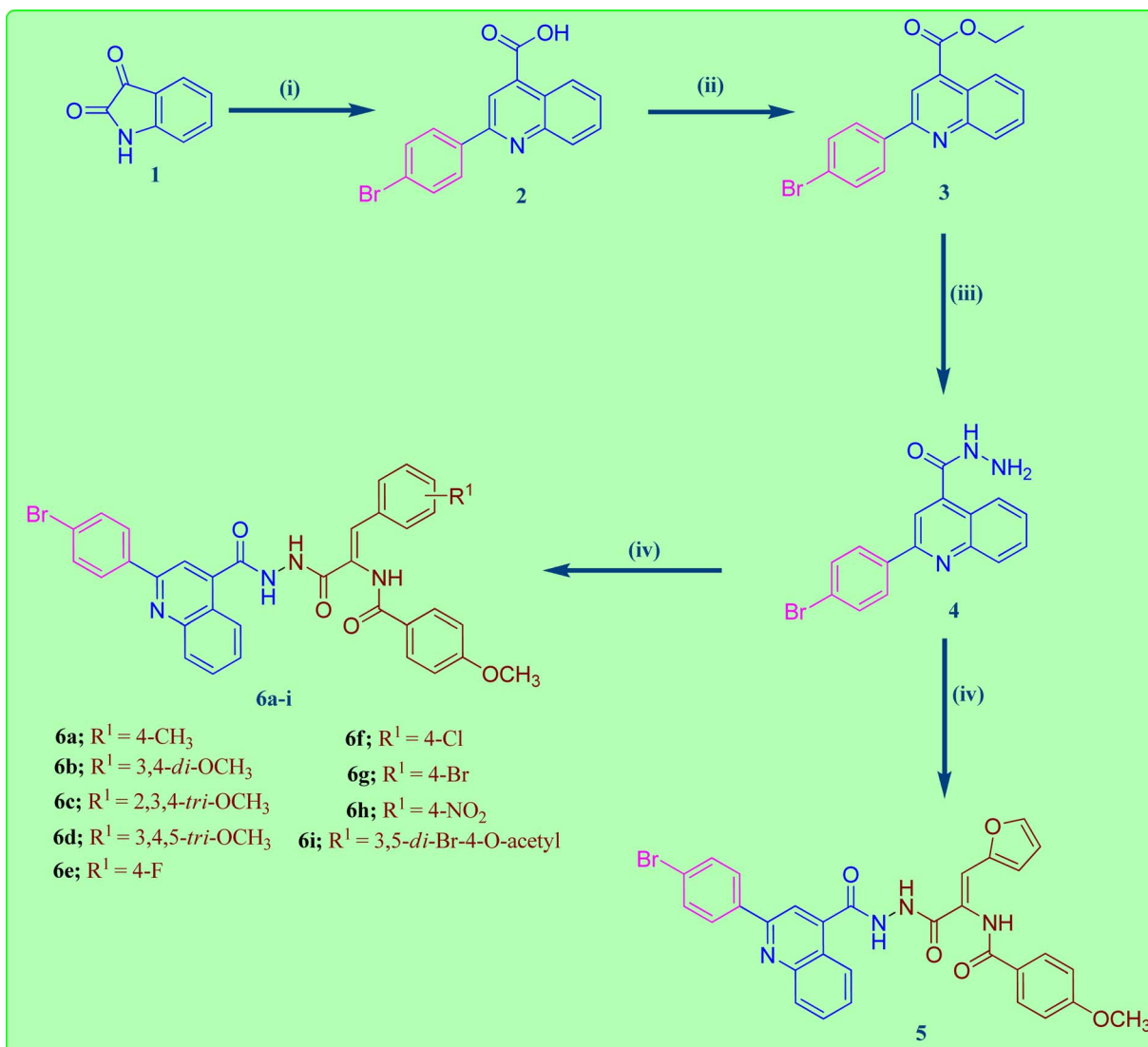
Based on these observations, we designed the synthesis of new set of quinoline-acrylamide hybrids 5 and 6a–i to be checked for their cytotoxic potential and EGFR kinase inhibition. The target derivatives will incorporate both quinoline-4-carbohydrazide structure as apoptosis inducer<sup>29</sup> connected to 3-arylacrylamide moiety, which was reported to efficiently inhibit kinase receptor<sup>30,31</sup> (Fig. 1). Furthermore, cell cycle and apoptosis activation will be determined for the most active hybrid to give idea about the phase at which these new hybrids halt the growth of cancer cells. Lastly, to further confirm apoptosis induction by the most active member, the treated

cancer cells were subjected to qRT-PCR measurements to quantify the level of apoptotic markers such p53 and effector caspase 9 compared to DMSO controls.

## 2. Results and discussion

### 2.1. Chemistry

The reaction sequences employed for the preparation of the target quinoline-4-carbohydrazide-acrylamide hybrids are illustrated in Scheme 1. Commercially available Istatin molecule **1** was utilized for the synthesis of quinoline-4-carboxylic acid **2** *via* its reaction with 4-bromoacetophenone and 33% potassium hydroxide following a previously reported procedure by heating the reactants at reflux in the existence of ethanol.<sup>32</sup> The key ethyl quinoline-4-carboxylate was prepared by reaction of quinoline-4-carboxylic acid **2** and ethanol in the existence of catalytic amount of Conc. H<sub>2</sub>SO<sub>4</sub>.<sup>33</sup> In the present study, the quinoline-4-carbohydrazinyl intermediate **4** was prepared through condensation of ethyl quinoline-4-carboxylate with hydrazine *via* heating the reactants at reflux in the existence of ethanol.<sup>34</sup> The target 2-(quinoline-4-carbonyl)hydrazide-acrylamide hybrids **5** and **6a–i** were synthesized through the reaction of quinoline-4-carbohydrazinyl intermediate **4** with the respective ethyl(Z)-3-aryl-2-(4-methoxybenzamido)acrylate derivative in the existence of ethanol and catalytic quantities of anhydrous sodium acetate. The structures of novel 2-(quinoline-4-carbonyl)hydrazide-acrylamide hybrids **5** and **6a–i** were authenticated by using spectral techniques (<sup>1</sup>H-NMR and <sup>13</sup>C-NMR). For instance, the <sup>1</sup>H-NMR spectrum of 2-(quinoline-4-carbonyl)hydrazide-3-(4-chlorophenyl)acrylamide hybrid **6f** as



**Scheme 1** Synthesis of the target 2-(quinoline-4-carbonyl)hydrazide-acrylamide hybrids 5 and 6a–i. Reagents: (i) 4-Br-C<sub>6</sub>H<sub>4</sub>COCH<sub>3</sub>, 33% KOH, C<sub>2</sub>H<sub>5</sub>OH, reflux 12 h; (ii) C<sub>2</sub>H<sub>5</sub>OH, Conc. H<sub>2</sub>SO<sub>4</sub>, reflux 12 h; (iii) NH<sub>2</sub>NH<sub>2</sub>, C<sub>2</sub>H<sub>5</sub>OH, reflux 7 h; (iv) respective 2-(4-methoxybenzamido) carboxylate, NaOAc, C<sub>2</sub>H<sub>5</sub>OH, reflux 18 h.

example, confirmed the presence of three amide NH groups through the existence of three broad singlet peaks at  $\delta_{\text{H}}$  10.81, 10.54 and 9.98 ppm. In addition to the presence of singlet peak at  $\delta_{\text{H}}$  7.36 ppm attributed to C2–H of acrylamide group. Moreover, the <sup>1</sup>H-NMR spectrum of 2-(quinoline-4-carbonyl)hydrazide-3-(4-chlorophenyl)acrylamide 6f showed a characteristic doublet signal at  $\delta_{\text{H}}$  8.44 ppm for the C5–H proton. Additionally, the presence of two triplet peaks at  $\delta_{\text{H}}$  7.88 and 7.71 ppm with integration of one proton each, disclosing to C7–H and C6–H of quinoline moiety, respectively. Also, the <sup>1</sup>H-NMR spectrum of 2-(quinoline-4-carbonyl)hydrazide-3-(4-chlorophenyl)acrylamide 6f indicated a singlet signals of three protons at  $\delta_{\text{H}}$  3.86 ppm pointing to the existence of methoxy group of the 4-methoxybenzamide moiety. Also, the structure of 2-(quinoline-4-carbonyl)hydrazide-3-(4-chlorophenyl)acrylamide 6f was authenticated by <sup>13</sup>C-NMR technique which

showed the presence of new shielded peak at  $\delta_{\text{C}}$  55.93 ppm attributed to the methoxy carbon (OCH<sub>3</sub>). In addition, the aromatic and acrylamide carbon atoms showed up in the aromatic region at 114.02–148.30 ppm. In addition, the characteristic C2 quinoline carbon was displayed in the <sup>13</sup>C-NMR spectrum at  $\delta_{\text{C}}$  155.01 ppm. Moreover, the three amide carbonyls of quinolinecarbohydrazide, acrylamide and 4-methoxybenzamide moieties were appeared in the <sup>13</sup>C-NMR spectrum of 2-(quinoline-4-carbonyl)hydrazide-3-(4-chlorophenyl)acrylamide 6f at  $\delta_{\text{C}}$  165.10, 165.98 and 166.13 ppm, respectively.

## 2.2. Biological evaluation

**2.2.1. Cytotoxic activity against MCF-7 cells.** In this study, all targeted 2-(quinoline-4-carbonyl)hydrazide-acrylamide hybrids 5 and 6a–i have been designed and their cytotoxic

**Table 1** Antiproliferative activity of synthesized 2-(quinoline-4-carbonyl)hydrazide-acrylamide hybrids 5 and 6a–i versus MCF-7 cell line. Results indicate mean  $\pm$  SD,  $n = 3$

Comp. no.	Ar	IC <sub>50</sub> ( $\mu$ M)
		MCF-7
5	Furan-2-yl	12.47 $\pm$ 0.40
6a	4-CH <sub>3</sub> -C <sub>6</sub> H <sub>4</sub> -	3.39 $\pm$ 0.11
6b	3,4-Di-OCH <sub>3</sub> -C <sub>6</sub> H <sub>3</sub> -	5.94 $\pm$ 0.17
6c	2,3,4-Tri-OCH <sub>3</sub> -C <sub>6</sub> H <sub>2</sub> -	51.77 $\pm$ 1.54
6d	3,4,5-Tri-OCH <sub>3</sub> -C <sub>6</sub> H <sub>2</sub> -	17.10 $\pm$ 0.55
6e	4-F-C <sub>6</sub> H <sub>4</sub> -	21.18 $\pm$ 0.68
6f	4-Cl-C <sub>6</sub> H <sub>4</sub> -	26.01 $\pm$ 0.84
6g	4-Br-C <sub>6</sub> H <sub>4</sub> -	39.13 $\pm$ 1.26
6h	4-NO <sub>2</sub> -C <sub>6</sub> H <sub>4</sub> -	2.71 $\pm$ 0.09
6i	3,5-Di-Br-4-OAcetyl-C <sub>6</sub> H <sub>2</sub> -	8.77 $\pm$ 0.28
Dox	—	6.18 $\pm$ 0.20

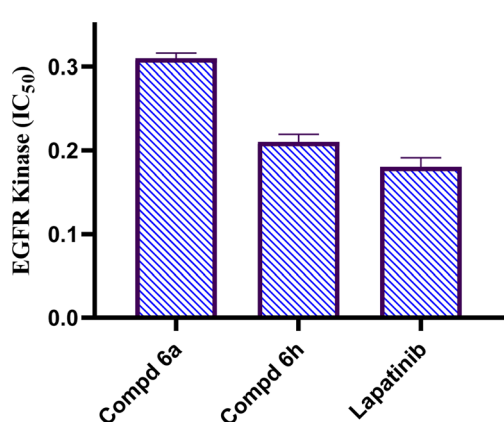


**Fig. 2** Results of EGFR-TK inhibition test as IC<sub>50</sub> result ( $\mu$ M) of tested 2-(quinoline-4-carbonyl)hydrazide-acrylamide derivatives 6a, 6h and lapatinib.

potential was examined *in vitro* against MCF-7 breast carcinoma cell line. The MTT colorimetric technique was used to evaluate the cytotoxic nature of these hybrids, with the widely utilized chemotherapeutic agent Doxorubicin (Dox) as reference control. The obtained IC<sub>50</sub> results were compared with Dox, as presented in Table 1. The collected results demonstrated that all the tested 2-(quinoline-4-carbonyl)hydrazide-acrylamide hybrids 5 and 6a–i hybrids except 6c showed modest to significant cytotoxic impact on the tested breast carcinoma with IC<sub>50</sub> that are ranged from 2.71–39.13  $\mu$ M. In general, four hybrids 6a, 6b, 6h and 6i displayed significant cytotoxic effect against the

examined cell line with IC<sub>50</sub> that are ranged from 2.71–8.77  $\mu$ M; in particular 2-(quinoline-4-carbonyl)hydrazide-3-(4-nitrophenyl)acrylamide 6h was the most potent hybrid with IC<sub>50</sub> value of 2.71  $\mu$ M compared to Dox (IC<sub>50</sub> = 6.18  $\mu$ M). Considering acrylamide moiety bearing phenyl group with halogen substituent at C3 position of acrylamide, a substantial drop in the cytotoxic activity was showed in compounds 6e, 6f and 6g which contain fluorine, chlorine and bromine group, which demonstrated modest IC<sub>50</sub> value of 21.18, 26.01 and 39.13  $\mu$ M, respectively against the tested cell line compared to Dox (IC<sub>50</sub> = 6.18  $\mu$ M). In addition, the replacement of the 4-Br substituent with 3,5-di-Br-4-acetoxyphenyl moiety 6i (IC<sub>50</sub> = 8.77  $\mu$ M) resulted in an increase of the biological activity. Furthermore, the activity intensified to became potent with the aryl group carrying electron donating substituent at C3 position of acrylamide moiety in 2-(quinoline-4-carbonyl)hydrazide-3-(4-methylphenyl)acrylamide 6a (IC<sub>50</sub> = 3.39  $\mu$ M) and 2-(quinoline-4-carbonyl)hydrazide-3-(3,4-dimethoxyphenyl)acrylamide 6b (IC<sub>50</sub> = 5.94  $\mu$ M) having 4-methyl and 3,4-dimethoxyphenyl group, respectively. On the other hand, compound 6d (IC<sub>50</sub> = 17.10  $\mu$ M) with 3,4,5-trimethoxyphenyl moiety resulted in a decrease in activity with one third the cytotoxic activity as Dox (IC<sub>50</sub> = 6.18  $\mu$ M). Alternatively, 2-(quinoline-4-carbonyl)hydrazide-acrylamide hybrid 5 (IC<sub>50</sub> = 12.47  $\mu$ M) bearing furan ring on C3 of acrylamide moiety elicited half the cytotoxic activity as Dox (IC<sub>50</sub> = 6.18  $\mu$ M).

**2.2.2. EGFR-TK inhibition assay.** The EGFR regulates information for signal transduction in a variety of biological processes, including cell proliferation, during division, and apoptosis activation.<sup>35</sup> Inhibitors of small molecules are useful for targeting EGFR-TK signalling in the initiation and advancement of cancer disease.<sup>36</sup> Therefore, EGFR-TK inhibitors have emerged as a promising area for drug creation and research study.<sup>37</sup> To provide mechanistic understanding of the anticancer potential of the most active hybrids, 2-(quinoline-4-carbonyl)hydrazide-acrylamide hybrids; 6a and 6h revealing the highest cytotoxic activity against breast carcinoma cell line, they were examined for their EGFR-TK inhibition activities. Results obtained as an IC<sub>50</sub> ( $\mu$ M) are presented in Fig. 2. 2-(Quinoline-4-carbonyl)hydrazide-3-(4-nitrophenyl)acrylamide 6h was the strongest inhibitor against EGFR with an IC<sub>50</sub> value of 0.22  $\mu$ M which is nearly equipotent to standard drug Lapatinib (IC<sub>50</sub> value of 0.18  $\mu$ M). The other compound; 2-(quinoline-4-carbonyl)hydrazide-3-(4-methylphenyl)acrylamide 6a possessed mild inhibitory activity against EGFR with IC<sub>50</sub> value of 0.31  $\mu$ M. Depending on the outputs of cytotoxic activity and EGFR kinase inhibition, 2-(quinoline-4-carbonyl)hydrazide-3-(4-nitrophenyl)acrylamide 6h was selected for further mechanistic investigations.

**2.2.3. Cell cycle analysis.** It is well documented that most tyrosine kinase inhibitors exert strong antiproliferative and pro-apoptotic effect.<sup>38</sup> In this regard, to evaluate the molecular mechanism of action, the cellular and biochemical effects of 2-(quinoline-4-carbonyl)hydrazide-acrylamide hybrid with highest cytotoxicity were studied; *i.e.* 6h bear 4-nitrophenyl moiety at the position 3 of acrylamide moiety. Flow cytometric assessments of the life cycle in MCF-7 cells that have been treated with



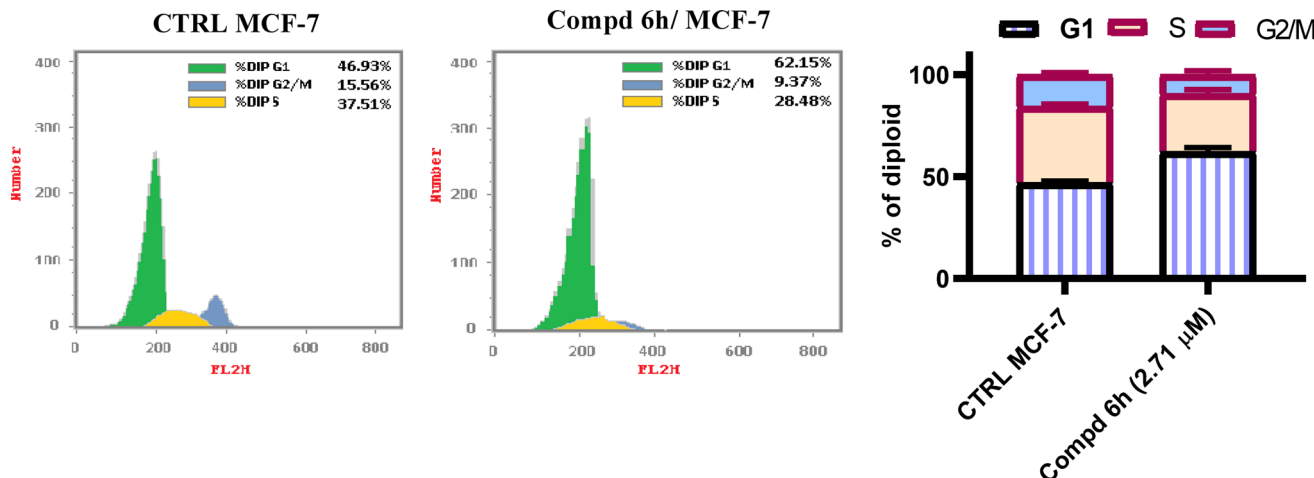


Fig. 3 2-(Quinoline-4-carbonyl)hydrazide-3-(4-nitrophenyl)acrylamide **6h** alters cellular cycle distribution in MCF-7 cells treated with 2.71  $\mu$ M of compound **6h** and compared to DMSO controls.

2-(quinoline-4-carbonyl)hydrazide-3-(4-nitrophenyl)acrylamide **6h** at the IC<sub>50</sub> concentration (IC<sub>50</sub> = 2.71  $\mu$ M) revealed a significant alterations in cellular cycle distribution, with considerable accumulation of cells in G1 phase and a decrease of both S and G2/M phases populations. It is notable that, the proportion of G1 phase was increased from 46.93% to 62.15% compared to DMSO untreated control group (Fig. 3). On the other hand, the percentage of S and G2/M phases was decreased from 37.51 and 15.56% to 28.48 and 9.37%, respectively for DMSO untreated control group. These findings are in agreement with the previously observed for EGFR-TK structural analogues.<sup>39</sup>

**2.2.4. Apoptosis staining assay.** To investigate whether compound **6h** could induce apoptosis, the apoptosis impact of 2-(quinoline-4-carbonyl)hydrazide-3-(4-nitrophenyl)acrylamide **6h** and DMSO (control untreated) were examined using

Annexin V FITC/PI double colouring assay. MCF-7 cells received treatment with compound **6h** at the concentration of 2.71  $\mu$ M for 48 h, then labelled with Annexin V FITC and PI dyes and assessed by flow cytometry. The results of flow cytometric measurements of apoptotic distribution effect in MCF-7 cells treated with 2-(quinoline-4-carbonyl)hydrazide-3-(4-nitrophenyl)acrylamide **6h** revealed that the tested compound could increase the percentage in the secondary cellular apoptosis from 0.11 to 17.78% compared to DMSO control. In addition, an increase in the primary apoptotic cells was also observed. It is noteworthy that, the percentage of primary apoptosis was rise from 0.39 to 9.55% as compared to DMSO control (Fig. 4). According to these findings, it could be concluded that this set of compounds could halt MCF-7 cells in G1 phase and provoke apoptotic cellular death.

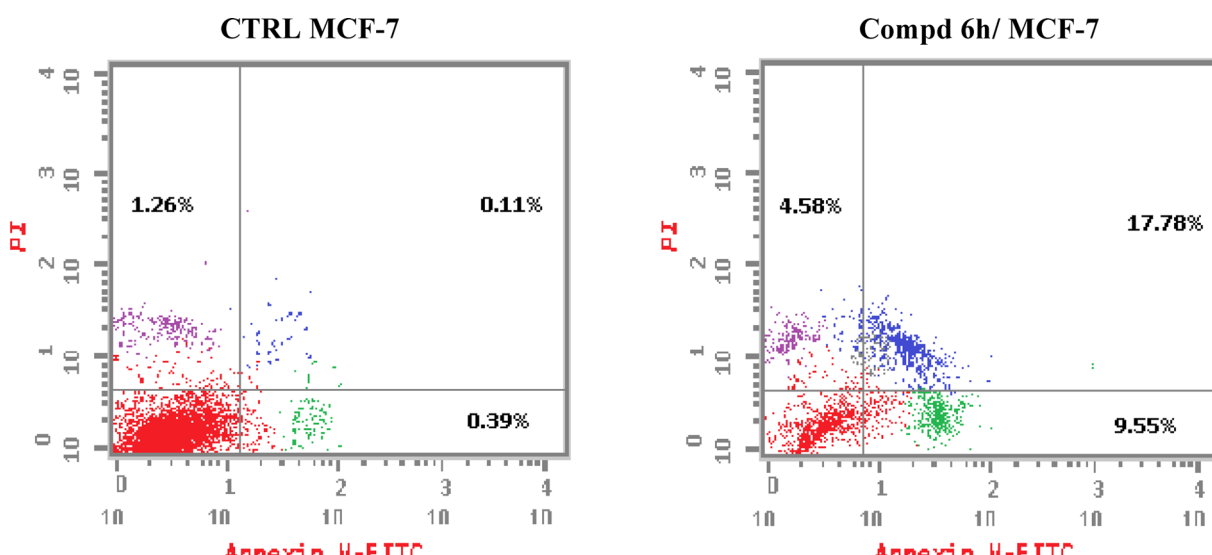


Fig. 4 2-(Quinoline-4-carbonyl)hydrazide-3-(4-nitrophenyl)acrylamide **6h** provoke apoptotic process in the examined MCF-7 cells after treatment with 2.71  $\mu$ M of compound **6h** and compared to DMSO controls.



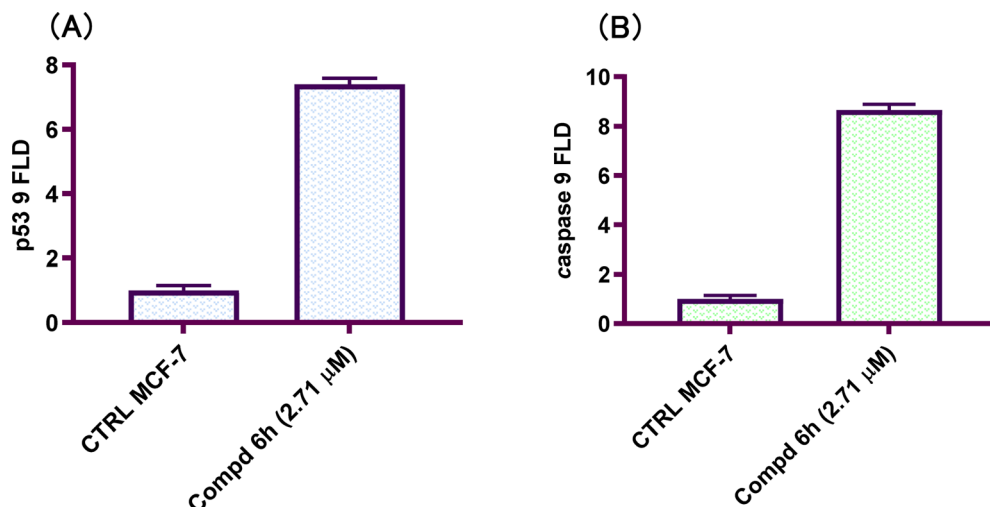


Fig. 5 2-(Quinoline-4-carbonyl)hydrazide-3-(4-nitrophenyl)acrylamide **6h** mediate p53 and caspase 9 expression. MCF-7 cells were treated with 2.71  $\mu$ M of tested hybrid for 48 h before qRT-PCR measurement and compared to untreated controls. (A) p53 level; (B) caspase 9 level.

**2.2.5. Apoptotic markers determination.** p53 is a transcription factor that both initiates and suppresses a number of target genes involved in cancer progression and apoptosis.<sup>40</sup> The p53 protein level increase during cellular stress and cytotoxic drugs by increased transcription or increased stability due to post-translational modifications such as phosphorylation.<sup>41</sup> The ability of p53 to modulate caspase activation and apoptosis induction is critical to its role as tumor suppressor.<sup>42</sup> Coordinately, p53 activation promotes the loss of mitochondrial potential ultimately leading to caspase activation and apoptosis.<sup>43</sup> To determine the downstream effects of EGFR tyrosine kinase inhibition by 2-(quinoline-4-carbonyl)hydrazide-3-(4-nitrophenyl)acrylamide **6h**, the level of tumor suppressor p53 and initiator caspase 9 proteins was examined by qRT-PCR. An increase in the level of p53 was detected in the tested cell line compared with controls at 48 h. The increased expression of p53 level was coupled with increase in the level of caspase 9 in compound **6h**-treated MCF-7 cell line at 48 h. The levels of p53 and caspase 9 were increased by 7.4- and 8.7-fold, respectively compared with controls (Fig. 5). In conclusions, 2-(quinoline-4-carbonyl)hydrazide-3-(4-nitrophenyl)acrylamide **6h** showed a pro-apoptotic effect through increasing p53 protein level and the level of initiator caspase 9 which support the results obtained from cell cycle and apoptosis staining examinations.

### 3. Conclusion

In conclusions, a new set of 2-(quinoline-4-carbonyl)hydrazide scaffold bearing acrylamide derivatives **5** and **6a-i** was synthesized and assessed for their *in vitro* antiproliferative activity against MCF-7 breast carcinoma cell line. Most tested hybrids revealed significant antiproliferative activity. Among them, three 2-(quinoline-4-carbonyl)hydrazide-acrylamide molecules; **6a**, **6b** and **6h** presented potent antiproliferative activity against the examined cell line with  $IC_{50}$  results of 3.39, 5.94 and 2.71

$\mu$ M, respectively, which were more potent than the reference compound Dox ( $IC_{50}$  = 6.18  $\mu$ M). For the most potent hybrids, 2-(quinoline-4-carbonyl)hydrazide-3-(4-methylphenyl)acrylamide **6a**, and 2-(quinoline-4-carbonyl)hydrazide-3-(4-nitrophenyl)acrylamide **6h** were examined for their inhibitory action against EGFR kinase and results revealed the responsiveness of EGFR-kinase to the tested hybrids with  $IC_{50}$  value of 0.31 and 0.22  $\mu$ M, respectively compared to Lapatinib ( $IC_{50}$  value of 0.18  $\mu$ M). The cell cycle analysis gave evident that 2-(quinoline-4-carbonyl)hydrazide-3-(4-nitrophenyl)acrylamide **6h** halted the MCF-7 at the G1 phase (1.3-fold more than DMSO controls) and provoke apoptosis (accumulation of cells by almost 18.1-fold compared with DMSO controls). As shown from the impacts on the gene expression of p53 and initiator caspase 9, compound **6h** boosted the expression of p53 and caspase 9 by 7.4- and 8.7-fold, respectively compared to DMSO controls. On the basis of the aforementioned findings, 2-(quinoline-4-carbonyl)hydrazide-3-(4-nitrophenyl)acrylamide **6h** could be considered as EGFR-TK inhibitor and fruitful clue for the development of novel antitumor agents against breast carcinoma.

## 4. Experimental

### 4.1. Chemistry

**4.1.1. Procedure for the synthesis of the (Z)-N-(1-aryl-3-(2-(2-(4-bromophenyl)quinoline-4-carbonyl)hydrazinyl)-3-oxoprop-1-en-2-yl)-4-methoxybenzamides **5** and **6a-i**.** To stirred suspension of 2-(quinoline-4-carbonyl)hydrazide **4** (3.42 g, 0.01 mol) in glacial acetic acid (25 mL), an equimolar quantity of respective ethyl (Z)-3-aryl-2-(4-methoxybenzamido)acrylate (0.01 mol) was refluxed along with anhydrous sodium acetate (1.07 g, 0.013 mol) for 18 h. After reaction completion, the mixture was placed into ice-cold water and vigorously agitated. Solid so obtained was filtered and rinsed three times with 5 mL of water each. The crude product was then dried in a desiccator and refined by flash chromatography with a mobile phase of ethyl



acetate/n-hexane (4 : 1) to attain pure 2-(quinoline-4-carbonyl) hydrazide-acrylamide hybrids 5 and **6a–i**.

**4.1.1.1. (Z)-N-(3-(2-(4-Bromophenyl)quinoline-4-carbonyl) hydrazinyl)-1-(furan-2-yl)-3-oxoprop-1-en-2-yl)-4-methoxybenzamide (5).** Yield (4.40 g, 72%); m.p. 257–259 °C;  $C_{31}H_{23}BrN_4O_5$  (611.44);  $^1H$ -NMR (400 MHz, DMSO- $d_6$ )  $\delta$ : 10.79 (s, 1H, NH), 10.46 (s, 1H, NH), 9.84 (s, 1H, NH), 8.43 (d,  $J$  = 8.5 Hz, 1H, Ar), 8.27 (d,  $J$  = 8.2 Hz, 2H, Ar), 8.17 (d,  $J$  = 9.5 Hz, 2H, Ar), 8.08 (d,  $J$  = 8.2 Hz, 2H, Ar), 7.88 (t,  $J$  = 7.7 Hz, 1H, Ar), 7.82 (s, 2H, Ar), 7.80 (s, 1H, Ar), 7.76–7.66 (m, 1H, Ar), 7.31 (s, 1H, =CH), 7.09 (d,  $J$  = 8.3 Hz, 2H, Ar), 6.79 (d,  $J$  = 3.5 Hz, 1H, Ar), 6.63 (dd,  $J$  = 3.6, 1.9 Hz, 1H, Ar), 3.87 (s, 3H, Ar-OCH<sub>3</sub>).  $^{13}C$ -NMR (101 MHz, DMSO)  $\delta$ : 166.11, 165.78, 164.60, 162.47, 155.01, 150.10, 148.30, 145.26, 142.01, 137.75, 132.46, 131.06, 130.42, 129.98, 129.75, 127.98, 126.56, 126.54, 126.03, 124.23, 124.06, 119.02, 117.15, 114.84, 113.99, 112.87, 55.92. MS ( $m/z$ , %): 611.50 ( $M^+$ , 31.38), 213.48 (100). Anal. calcd (%): C, 60.988; H, 4.39; N, 7.87; found (%): C, 60.94; H, 4.26; N, 7.71.

**4.1.1.5. (Z)-N-(3-(2-(4-Bromophenyl)quinoline-4-carbonyl) hydrazinyl)-3-oxo-1-(3,4,5-trimethoxyphenyl)prop-1-en-2-yl)-4-methoxybenzamide (6d).** Yield (4.55 g, 64%); m.p. 208–210 °C;  $C_{36}H_{31}BrN_4O_7$  (711.56);  $^1H$ -NMR (400 MHz, DMSO- $d_6$ )  $\delta$  10.77 (s, 1H, NH), 10.46 (s, 1H, NH), 9.92 (s, 1H, NH), 8.44 (d,  $J$  = 8.4 Hz, 1H), 8.28–8.23 (m, 2H), 8.18–8.13 (m, 2H), 8.08 (d,  $J$  = 8.5 Hz, 2H), 7.87 (ddd,  $J$  = 8.4, 6.8, 1.5 Hz, 1H), 7.83–7.78 (m, 2H), 7.70 (ddd,  $J$  = 8.2, 6.8, 1.2 Hz, 1H), 7.43 (s, 1H, =CH), 7.09–7.04 (m, 2H), 7.02 (s, 2H), 3.84 (s, 3H, OCH<sub>3</sub>), 3.67 (s, 3H, OCH<sub>3</sub>), 3.63 (s, 6H, 2OCH<sub>3</sub>).  $^{13}C$ -NMR (101 MHz, DMSO)  $\delta$ : 166.11, 165.99, 165.09, 162.49, 155.01, 153.07, 148.31, 142.09, 138.65, 137.77, 132.46, 131.50, 131.06, 130.37, 129.98, 129.82, 129.75, 128.41, 127.94, 126.30, 126.06, 124.22, 124.09, 117.12, 113.91, 107.70, 60.54, 56.09, 55.91. MS ( $m/z$ , %): 711.38 ( $M^+$ , 19.20), 95.23 (100). Anal. calcd (%): C, 60.77; H, 4.39; N, 7.87; found (%): C, 60.94; H, 4.51; N, 7.66.

**4.1.1.6. (Z)-N-(3-(2-(4-Bromophenyl)quinoline-4-carbonyl) hydrazinyl)-1-(4-fluorophenyl)-3-oxoprop-1-en-2-yl)-4-methoxybenzamide (6e).** Yield (4.86 g, 76%); m.p. 258–260 °C;  $C_{33}H_{24}BrFN_4O_4$  (639.47);  $^1H$ -NMR (400 MHz, DMSO- $d_6$ )  $\delta$  10.78 (s, 1H, NH), 10.50 (s, 1H, NH), 9.95 (s, 1H, NH), 8.45 (d,  $J$  = 8.4 Hz, 1H), 8.30–8.24 (m, 2H), 8.17 (d,  $J$  = 8.1 Hz, 2H), 8.05 (d,  $J$  = 8.5 Hz, 2H), 7.88 (ddd,  $J$  = 8.5, 6.8, 1.4 Hz, 1H), 7.84–7.78 (m, 2H), 7.73 (d,  $J$  = 2.9 Hz, 1H), 7.71 (s, 1H), 7.69 (dd,  $J$  = 3.6, 2.3 Hz, 1H), 7.40 (s, 1H, =CH), 7.29–7.22 (m, 2H), 7.12–7.05 (m, 2H), 3.86 (s, 3H, OCH<sub>3</sub>).  $^{13}C$ -NMR (101 MHz, DMSO)  $\delta$ : 166.11, 166.01, 165.10, 162.54, 161.29, 155.01, 148.31, 142.11, 137.77, 132.45, 132.12, 131.15, 131.04, 130.44, 129.98, 129.74, 129.52, 129.17, 127.95, 126.27, 126.06, 124.22, 124.09, 117.13, 116.16, 114.00, 55.93. MS ( $m/z$ , %): 639.18 ( $M^+$ , 23.38), 486.00 (100). Anal. calcd (%): C, 61.98; H, 3.78; N, 8.76; found (%): C, 62.09; H, 3.88; N, 8.67.

**4.1.1.7. (Z)-N-(3-(2-(4-Bromophenyl)quinoline-4-carbonyl) hydrazinyl)-1-(4-chlorophenyl)-3-oxoprop-1-en-2-yl)-4-methoxybenzamide (6f).** Yield (5.37 g, 82%); m.p. 276–278 °C;  $C_{33}H_{24}BrClN_4O_4$  (655.93);  $^1H$ -NMR (400 MHz, DMSO- $d_6$ )  $\delta$  10.81 (s, 1H, NH), 10.54 (s, 1H, NH), 9.98 (s, 1H, NH), 8.44 (dd,  $J$  = 8.4, 1.4 Hz, 1H), 8.27 (d,  $J$  = 8.5 Hz, 2H), 8.17 (d,  $J$  = 8.5 Hz, 2H), 8.07–8.01 (m, 2H), 7.88 (t,  $J$  = 6.8 Hz, 1H), 7.80 (dd,  $J$  = 8.9, 2.3 Hz, 2H), 7.71 (t,  $J$  = 6.8 Hz, 1H), 7.68–7.63 (m, 2H), 7.51–7.44 (m, 2H), 7.36 (s, 1H, =CH), 7.12–7.05 (m, 2H), 3.86 (s, 3H, OCH<sub>3</sub>).  $^{13}C$ -NMR (101 MHz, DMSO)  $\delta$ : 166.13, 165.98, 165.10, 162.57, 155.01, 148.30, 142.01, 137.75, 133.74, 133.53, 132.45, 131.59, 131.06, 130.46, 130.10, 129.98, 129.75, 129.10, 129.06, 127.98, 126.21, 126.01, 124.23, 124.07, 117.14, 114.02, 55.93. MS ( $m/z$ , %): 655.05 ( $M^+$ , 10.76), 75.80 (100). Anal. calcd (%): C, 60.43; H, 3.69; N, 8.54; found (%): C, 60.40; H, 3.84; N, 8.68.

**4.1.1.8. (Z)-N-(1-(4-Bromophenyl)-3-(2-(4-bromophenyl)quinoline-4-carbonyl)hydrazinyl)-3-oxoprop-1-en-2-yl)-4-methoxybenzamide (6g).** Yield (5.53 g, 79%); m.p. 261–263 °C;



$C_{33}H_{24}Br_2N_4O_4$  (700.38);  $^1H$ -NMR (400 MHz, DMSO- $d_6$ )  $\delta$  10.81 (s, 1H, NH), 10.54 (s, 1H, NH), 9.97 (s, 1H, NH), 8.43 (d,  $J$  = 8.4 Hz, 1H), 8.27 (d,  $J$  = 8.4 Hz, 2H), 8.17 (d,  $J$  = 8.6 Hz, 2H), 8.03 (d,  $J$  = 8.4 Hz, 2H), 7.88 (t,  $J$  = 7.7 Hz, 1H), 7.81 (d,  $J$  = 8.2 Hz, 2H), 7.72 (q,  $J$  = 8.4, 7.5 Hz, 2H), 7.60 (t,  $J$  = 6.7 Hz, 3H), 7.33 (s, 1H, =CH), 7.08 (d,  $J$  = 8.4 Hz, 2H), 3.86 (s, 3H, OCH<sub>3</sub>).  $^{13}C$ -NMR (101 MHz, DMSO)  $\delta$ : 166.13, 165.98, 165.10, 162.57, 155.01, 148.30, 142.01, 137.75, 133.74, 133.53, 132.45, 131.59, 131.06, 130.46, 130.10, 129.98, 129.75, 129.10, 129.06, 127.98, 126.21, 126.01, 124.23, 124.07, 117.14, 114.02, 55.93. MS ( $m/z$ , %): 700.27 (M<sup>+</sup>, 13.24), 509.29 (100). Anal. calcd (%): C, 56.59; H, 3.45; N, 8.00; found (%): C, 56.48; H, 3.31; N, 7.86.

**4.1.1.9.** (*Z*)-*N*-(3-(2-(2-(4-Bromophenyl)quinoline-4-carbonyl)hydrazinyl)-1-(4-nitrophenyl)-3-oxoprop-1-en-2-yl)-4-methoxybenzamide (**6h**). Yield (5.33 g, 80%); m.p. 263–265 °C;  $C_{33}H_{24}BrN_5O_6$  (666.48);  $^1H$ -NMR (400 MHz, DMSO- $d_6$ )  $\delta$  10.88 (s, 1H, NH), 10.68 (s, 1H, NH), 10.14 (s, 1H, NH), 8.54 (d,  $J$  = 8.5 Hz, 1H), 8.43 (d,  $J$  = 8.3 Hz, 1H), 8.35 (d,  $J$  = 8.5 Hz, 1H), 8.29–8.24 (m, 3H), 8.17 (d,  $J$  = 7.2 Hz, 2H), 8.02 (d,  $J$  = 8.4 Hz, 2H), 7.87 (d,  $J$  = 8.2 Hz, 2H), 7.81 (d,  $J$  = 8.2 Hz, 2H), 7.72 (t,  $J$  = 7.8 Hz, 1H), 7.38 (s, 1H, =CH), 7.08 (d,  $J$  = 8.4 Hz, 2H), 3.86 (s, 3H, OCH<sub>3</sub>).  $^{13}C$ -NMR (101 MHz, DMSO)  $\delta$ : 166.13, 165.99, 164.88, 162.69, 155.02, 148.30, 147.17, 141.90, 141.66, 137.74, 132.83, 132.46, 131.08, 130.79, 130.54, 130.00, 129.75, 128.01, 127.04, 125.99, 124.24, 124.15, 124.04, 117.16, 115.55, 114.06, 55.96. MS ( $m/z$ , %): 666.71 (M<sup>+</sup>, 11.06), 552.28 (100). Anal. calcd (%): C, 59.47; H, 3.63; N, 10.51; found (%): C, 59.38; H, 3.74; N, 10.59.

**4.1.1.10.** (*Z*)-2,6-Dibromo-4-(3-(2-(2-(4-bromophenyl)quinoline-4-carbonyl)hydrazinyl)-2-(4-methoxybenzamido)-3-oxoprop-1-enyl)phenyl acetate (**6i**). Yield (5.94 g, 71%); m.p. 217–219 °C;  $C_{35}H_{25}Br_3N_4O_6$  (837.31);  $^1H$  NMR (400 MHz, DMSO- $d_6$ )  $\delta$  10.85 (s, 1H, NH), 10.62 (s, 1H, NH), 10.08 (s, 1H, NH), 8.44 (d,  $J$  = 8.4 Hz, 1H), 8.27 (dd,  $J$  = 8.6, 2.5 Hz, 2H), 8.17 (d,  $J$  = 7.9 Hz, 2H), 8.04 (s, 1H), 8.02 (d,  $J$  = 3.7 Hz, 3H), 7.88 (ddd,  $J$  = 8.5, 6.7, 1.5 Hz, 1H), 7.83–7.79 (m, 2H), 7.72 (t,  $J$  = 7.7 Hz, 1H), 7.35 (s, 1H), 7.09 (dd,  $J$  = 9.1, 2.5 Hz, 2H), 3.86 (s, 3H, OCH<sub>3</sub>), 2.41 (s, 3H, COCH<sub>3</sub>).  $^{13}C$ -NMR (101 MHz, DMSO)  $\delta$ : 167.67, 166.22, 166.09, 164.60, 162.64, 155.02, 148.31, 145.70, 141.93, 137.75, 135.74, 133.45, 132.45, 131.75, 131.06, 130.41, 130.00, 129.75, 128.00, 126.84, 126.08, 125.98, 124.24, 124.06, 117.63, 117.15, 114.05, 55.94, 20.66. MS ( $m/z$ , %): 837.34 (M<sup>+</sup>, 17.66), 238.16 (100). Anal. calcd (%): C, 50.21; H, 3.01; N, 6.69; found (%): C, 50.04; H, 2.91; N, 6.83.

#### 4.2. Biological studies

All the experimental procedure used in the biological studies were shown in the ESI.†

#### Data availability

The authors agree to reproduce any published material (figures, schemes, tables, or any extract of a text) that does not fall into the public domain, or for which they do not hold the copyright.

#### Conflicts of interest

No potential conflict of interest was reported by the author(s).

## Acknowledgements

This work was supported by the Deanship of Scientific Research, Vice Presidency for Graduate Studies and Scientific Research at King Faisal University, Saudi Arabia (Grant No. A490).

## References

- R. L. Siegel, K. D. Miller, N. S. Wagle and A. Jemal, Cancer statistics, 2023, *Ca-Cancer J. Clin.*, 2023, **73**, 17–48.
- G. Housman, S. Byler, S. Heerboth, K. Lapinska, M. Longacre, N. Snyder and S. Sarkar, Drug Resistance in Cancer: An Overview, *Cancers*, 2014, **6**, 1769–1792.
- M. Cai, X.-L. Song, X.-A. Li, M. Chen, J. Guo, D.-H. Yang, Z. Chen and S.-C. Zhao, Current therapy and drug resistance in metastatic castration-resistant prostate cancer, *Drug Resistance Updates*, 2023, **68**, 100962.
- Y. Xiao, P. Liu, J. Wei, X. Zhang, J. Guo and Y. Lin, Recent progress in targeted therapy for non-small cell lung cancer, *Front. Pharmacol.*, 2023, **14**, 1125547.
- N. Ebrahimi, M. S. Manavi, F. Faghikhhorasani, S. S. Fakhr, F. J. Baei, F. F. Khorasani, M. M. Zare, N. P. Far, F. Rezaei-Tazangi, J. Ren, R. J. Reiter, N. Nabavi, A. R. Aref, C. Chen, Y. N. Ertas and Q. Lu, Harnessing function of EMT in cancer drug resistance: a metastasis regulator determines chemotherapy response, *Cancer Metastasis Rev.*, 2024, **43**, 457–479.
- S. Zhou, H. Xu, Y. Duan, Q. Tang, H. Huang and F. Bi, Survival mechanisms of circulating tumor cells and their implications for cancer treatment, *Cancer Metastasis Rev.*, 2024, **2**, 1–17.
- S. Wu, H. Zhu, Y. Wu, C. Wang, X. Duan and T. Xu, Molecular mechanisms of long noncoding RNAs associated with cervical cancer radiosensitivity, *Front. Genet.*, 2023, **13**, 1093549–1093562.
- C. Wang, Y. Zhang, T. Zhang, J. Xu, S. Yan, B. Liang and D. Xing, Epidermal growth factor receptor dual-target inhibitors as a novel therapy for cancer: A review, *Int. J. Biol. Macromol.*, 2023, **253**, 127440.
- J. Chen, F. Zeng, S. J. Forrester, S. Eguchi, M.-Z. Zhang and R. C. Harris, Expression and Function of the Epidermal Growth Factor Receptor in Physiology and Disease, *Physiol. Rev.*, 2016, **96**, 1025–1069.
- H. Liu, B. Zhang and Z. Sun, Spectrum of EGFR aberrations and potential clinical implications: insights from integrative pan-cancer analysis, *Cancer Commun.*, 2020, **40**, 43–59.
- S. Halder, S. Basu, S. P. Lall, A. K. Ganti, S. K. Batra and P. Seshacharyulu, Targeting the EGFR signaling pathway in cancer therapy: What's new in 2023?, *Expert Opin. Ther. Targets*, 2023, **27**, 305–324.
- S. M. Rodriguez, A. Kamel, G. V. Ciubotaru, G. Onose, A.-S. Sevastre, V. Sfredel, S. Danoiu, A. Dricu and L. G. Tataranu, An Overview of EGFR Mechanisms and Their Implications in Targeted Therapies for Glioblastoma, *Int. J. Mol. Sci.*, 2023, **24**, 11110–11133.
- S. Qian, Z. Wei, W. Yang, J. Huang, Y. Yang and J. Wang, The role of BCL-2 family proteins in regulating apoptosis and cancer therapy, *Front. Oncol.*, 2022, **12**, 985363–985376.



14 K. Oravetz, A.-V. Todea, O. Balacescu, D. Cruceriu and E. Rakosy-Tican, Potential antitumor activity of garlic against colorectal cancer: focus on the molecular mechanisms of action, *Eur. J. Nutr.*, 2023, **62**, 2347–2363.

15 V. Shoshan-Barmatz, T. Arif and A. Shteiinfer-Kuzmine, Apoptotic proteins with non-apoptotic activity: expression and function in cancer, *Apoptosis*, 2023, **28**, 730–753.

16 R.-J. Man, N. Jeehani, C. Zhou and Y.-S. Yang, Recent progress in the development of quinoline derivatives for the exploitation of anti-cancer agents, *Anti-Cancer Agents Med. Chem.*, 2021, **21**, 825–838.

17 M. Mohasin, M. Zafer Alam, Q. Ullah, A. Ahmad, P. F. Rahaman and S. A. Khan, A Review on Synthesis and Biological Applications of Quinoline Derivative as Fused Aromatic Compounds, *Polycyclic Aromat. Compd.*, 2024, **1**–30.

18 A. Saxena, S. Majee, D. Ray and B. Saha, Inhibition of cancer cells by Quinoline-Based compounds: A review with mechanistic insights, *Bioorg. Med. Chem.*, 2024, **103**, 117681–117693.

19 B. S. Matada, R. Pattanashettar and N. G. Yernale, A comprehensive review on the biological interest of quinoline and its derivatives, *Bioorg. Med. Chem.*, 2021, **32**, 115973.

20 M. Ryczkowska, N. Maciejewska, M. Olszewski, M. Witkowska and S. Makowiec, Tetrahydroquinolinone derivatives exert antiproliferative effect on lung cancer cells through apoptosis induction, *Sci. Rep.*, 2022, **12**, 19076.

21 M. S. Nafie, S. M. Kishk, S. Mahgoub and A. M. Amer, Quinoline-based thiazolidinone derivatives as potent cytotoxic and apoptosis-inducing agents through EGFR inhibition, *Chem. Biol. Drug Des.*, 2022, **99**, 547–560.

22 H. M. Abd El-Lateef, L. M. A. Ghany, R. M. Saleem, A. H. A. Maghrabi, M. A. Y. Alahdal, E. H. K. Ali, B. Y. Beshay, I. Zaki and R. E. Masoud, Design, synthesis and antiproliferative screening of newly synthesized coumarin-acrylamide hybrids as potential cytotoxic and apoptosis inducing agents, *RSC Adv.*, 2023, **13**, 32547–32557.

23 X. Hu, S. Tang, F. Yang, P. Zheng, S. Xu, Q. Pan and W. Zhu, Design, Synthesis, and Antitumor Activity of Olmutinib Derivatives Containing Acrylamide Moiety, *Molecules*, 2021, **26**, 3041–3054.

24 D. N. Binjawhar, F. A. Al-Salmi, O. A. A. Ali, M. A. Alghamdi, E. Fayad, R. M. Saleem, I. Zaki and N. Farouk, Design, synthesis and cytotoxic activity of molecular hybrids based on quinolin-8-yloxy and cinnamide hybrids and their apoptosis inducing property, *RSC Adv.*, 2024, **14**, 11443–11451.

25 D. Honglin, G. Chao, S. Xiaojie, Z. Yutong, W. Zhengjie, L. Limin, W. Tao, Z. Luye, Z. Yang, Y. Qin, Z. Peirong, S. Lihong and Z. Qiurong, Design, Synthesis, and Antitumor Activity Evaluation of 2,4,6-Trisubstituted Quinazoline Derivatives Containing Acrylamide, *Russ. J. Bioorg. Chem.*, 2022, **48**, 1089–1100.

26 V. Gunasekaran, R. Yuvakkumar, R. Ganesan, S. C. Palapetta and H. Gurusamy, Biological evaluation of polycyclic chalcone based acrylamides in human MCF-7 and HeLa cancer cell lines, *Environ. Res.*, 2023, **222**, 115395.

27 F. de Marinis, K. K. Laktionov, A. Poltoratskiy, I. Egorova, M. Hochmair, A. Passaro, M. R. Migliorino, G. Metro, M. Gottfried and D. Tsoi, Afatinib in EGFR TKI-naïve patients with locally advanced or metastatic EGFR mutation-positive non-small cell lung cancer: Interim analysis of a Phase 3b study, *Lung Cancer*, 2021, **152**, 127–134.

28 S.-C. Nao, L. Kong, D. S.-H. Chan, J. Liu, L.-S. Huang, L. Wu, J. Wu, C.-Y. Wong, W. Wang and C.-H. Leung, Covalent inhibition of epidermal growth factor receptor using a long-lived iridium(III)-afatinib probe, *Int. J. Biol. Macromol.*, 2024, **259**, 129211.

29 N. Ryad, A. A. Elmaaty, I. M Ibrahim, A. H. Ahmed Maghrabi, M. A. Yahya Alahdal, R. M. Saleem, I. Zaki and L. M. A. A. Ghany, Harnessing molecular hybridization approach to discover novel quinoline EGFR-TK inhibitors for cancer treatment, *Future Med. Chem.*, 2024, **16**, 1087–1107.

30 S. Ding, X. Dong, Z. Gao, X. Zheng, J. Ji, M. Zhang, F. Liu, S. Wu, M. Li, W. Song, J. Shen, W. Duan, J. Liu and Y. Chen, Design, synthesis and biological evaluation of novel N-(3-amino-4-methoxyphenyl)acrylamide derivatives as selective EGFRL858R/T790M kinase inhibitors, *Bioorg. Chem.*, 2022, **118**, 105471.

31 Z. Jiang, Y. Li, X. Zhou, J. Wen, P. Zheng and W. Zhu, Research progress on small molecule inhibitors targeting KRAS G12C with acrylamide structure and the strategies for solving KRAS inhibitor resistance, *Bioorg. Med. Chem.*, 2024, **100**, 117627.

32 H. M. Abd El-Lateef, A. A. Elmaaty, L. M. A. Abdel Ghany, M. S. Abdel-Aziz, I. Zaki and N. Ryad, Design and Synthesis of 2-(4-Bromophenyl)Quinoline-4-Carbohydrazide Derivatives via Molecular Hybridization as Novel Microbial DNA-Gyrase Inhibitors, *ACS Omega*, 2023, **8**, 17948–17965.

33 L. M. A. A. Ghany, N. Ryad, M. S. Abdel-Aziz, H. M. A. El-Lateef, I. Zaki and B. Y. Beshay, Design, synthesis, antimicrobial evaluation, and molecular modeling of new sulfamethoxazole and trimethoprim analogs as potential DHPS/DHFR inhibitors, *J. Mol. Struct.*, 2024, **1309**, 138170.

34 H. M. A. El-Lateef, R. M. Saleem, M. A. Bazuhair, A. H. A. Maghrabi, E. H. K. Ali, I. Zaki and R. E. Masoud, Design, synthesis and tubulin polymerization inhibition activity of newly synthesized hydrazone-linked to combretastatin analogues as potential anticancer agents, *J. Mol. Struct.*, 2023, **1292**, 136190.

35 R. Kobayashi, E. Hoshikawa, T. Saito, O. Suebsamarn, E. Naito, A. Suzuki, S. Ishihara, H. Haga, K. Tomihara and K. Izumi, The EGF/EGFR axis and its downstream signaling pathways regulate the motility and proliferation of cultured oral keratinocytes, *FEBS Open Bio*, 2023, **13**, 1469–1484.

36 T. Zubair and D. Bandyopadhyay, Small Molecule EGFR Inhibitors as Anti-Cancer Agents: Discovery, Mechanisms of Action, and Opportunities, *Int. J. Mol. Sci.*, 2023, **24**, 2651–2663.



37 R. Damare, K. Engle and G. Kumar, Targeting epidermal growth factor receptor and its downstream signaling pathways by natural products: A mechanistic insight, *Phytother. Res.*, 2024, **38**, 2406–2447.

38 R. Pal, G. Teli, G. S. P. Matada and P. S. Dhiwar, Designing strategies, structural activity relationship and biological activity of recently developed nitrogen containing heterocyclic compounds as epidermal growth factor receptor tyrosinase inhibitors, *J. Mol. Struct.*, 2023, **1291**, 136021.

39 T. Zhang, Y. Liang, P. Zuo, S. Jing, T. Li, Y. Wang, C. Lv, D. Li, J. Zhang and Z. Wei, 20(S)-Protopanaxadiol blocks cell cycle progression by targeting epidermal growth factor receptor, *Food Chem. Toxicol.*, 2020, **135**, 111017.

40 A. J. Levine, The many faces of p53: something for everyone, *J. Mol. Cell Biol.*, 2019, **11**, 524–530.

41 T. T. T. Phan, N. V. Truong, W.-G. Wu, Y.-C. Su, T.-S. Hsu and L.-Y. Lin, Tumor suppressor p53 mediates interleukin-6 expression to enable cancer cell evasion of genotoxic stress, *Cell Death Discovery*, 2023, **9**, 340.

42 O. Hassin and M. Oren, Drugging p53 in cancer: one protein, many targets, *Nat. Rev. Drug Discovery*, 2023, **22**, 127–144.

43 C. Xiong, H. Ling, Q. Hao and X. Zhou, Cuproptosis: p53-regulated metabolic cell death?, *Cell Death Differ.*, 2023, **30**, 876–884.